ELSEVIER

Polymer 41 (2000) 2319–2323

polymer

Polymer Communication

‘Ductile’ mixed biopolymer gel composites

K.P. Plucknett*, V. Normand, S.J. Pomfret, D. Ferdinando

Unilever Research, Colworth House, Sharnbrook, Bedfordshire, MK44 1LQ, UK

Received 23 July 1999; received in revised form 17 August 1999; accepted 19 August 1999

Abstract

The deformation and failure behaviour of novel ‘pseudo-ductile’ gelatin/maltodextrin mixed biopolymer gels have been assessed using dynamic mechanical tests, conducted on the stage of a confocal laser scanning microscope. These materials exhibit a phase-separated structure, with spherical *maltodextrin-rich* inclusions within a continuous *gelatin-rich* matrix. Using both conventional tension and notched compact tension tests, it was observed that the apparent ductility was due to inclusion/matrix interfacial debonding, resulting in reduced elastic modulus. Based upon a simple debonding model, an interfacial fracture energy of $\sim 0.25\ J\ m^{-2}$ was determined. © 1999 Elsevier Science Ltd. All rights reserved.

Keywords: Biopolymer gel composites; Maltodextrin; Gelatin

1. Introduction

Biopolymer gels have found widespread application in structured foods during the past decade. While it can therefore be envisaged that they are subjected to large deformation strains during processing or consumption, most examinations of their mechanical behaviour have focused upon small strain behaviour in shear [1]. Recent large deformation studies have therefore attempted to redress this balance [2]. In many real structured food applications, mixed biopolymer gels are utilised that exhibit typical emulsion-like phase separated microstructures, with spherical inclusions within a continuous matrix [3]. Currently, the deformation and failure response of these materials is not well understood. However, several attempts have been made to characterise and model the failure behaviour of analogous composite gels, with both rigid and deformable *included* particles, assuming either strong or weak interfacial bonding conditions between the particles and the matrix [4,5]. In the instance of a weak interfacial bond between the two phases, debonding can be anticipated when the particles have a significantly higher elastic modulus than the continuous matrix. Conversely, for a system with relatively strong interfacial bonding, fracture through the particles is likely. Failure can also occur near the interface, but slightly within the matrix (or particle), when there is a relatively strong interfacial bond and the included particles have a significantly higher elastic modulus than the matrix (or lower elastic modulus for failure within the particle). This behaviour is less common, but has been noted in composites comprised of agarose particles (5% (w/w)) in a considerably less stiff agarose matrix (1% (w/w)) [6].

The present work describes a preliminary study of the large strain deformation and failure behaviour of immiscible phase-separated gelatin/maltodextrin biopolymer gels. To elucidate the failure mechanisms that may be operating in these materials, emphasis has been placed upon dynamic observation of deformation and fracture by conducting tensile mechanical tests on a confocal laser scanning microscope (CLSM), which is an approach that has not been taken with these materials before.

2. Experimental section

Gelatin (LH1e, SKW Biosystem, Carentan, France) solutions were prepared by dissolving the powder in de-ionised water (0.1 M NaCl) at 60°C for 30 min, with sodium azide (500 ppm) addition to prevent bacteriological degradation. Sirius Red (500 ppm) was also added to fluorescently stain the gelatin for CLSM (MRC 600 CLSM (Bio-Rad Inc., Hemel Hempstead, UK) attached to an Ortholux microscope (Leica, Milton Keynes, UK)). Maltodextrin (SA2e, Avebe, UK) solutions were prepared by dissolving the powder at 98°C, for 30 min, in deionised water (0.1 M NaCl). Biopolymer mixtures were subsequently prepared by mixing the individual gelatin and maltodextrin solutions at 60°C. The mixed solution was then poured between glass plates,

* Corresponding author.

0032-3861/00/$ - see front matter © 1999 Elsevier Science Ltd. All rights reserved.
PII: S0032-3861(99)00602-3

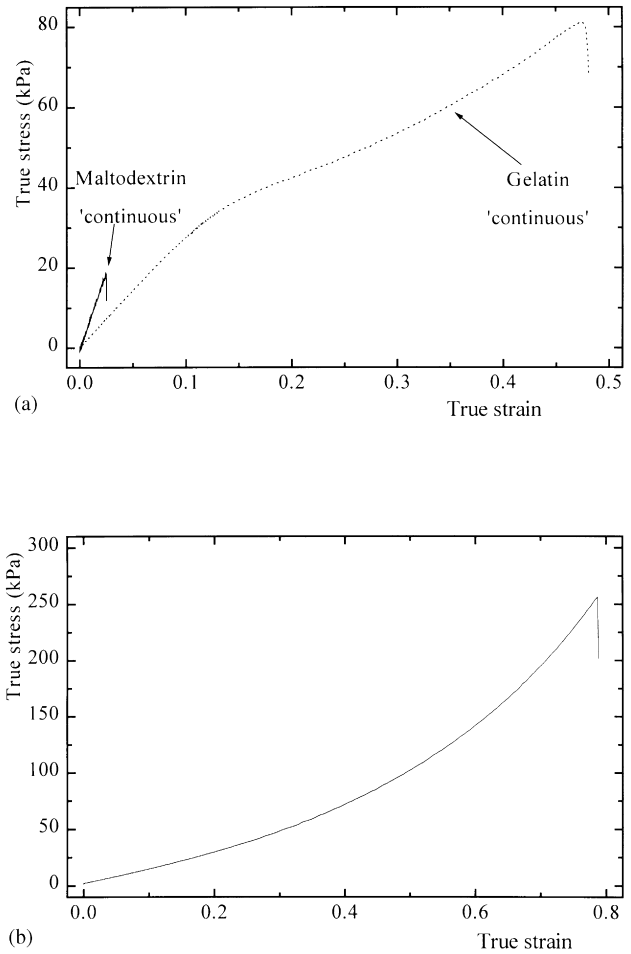

Fig. 1. (a) Typical true stress/true strain curves for both maltodextrin (4.6% (w/w) gelatin/20% (w/w) maltodextrin) and gelatin continuous (12% (w/w) gelatin/12% (w/w) maltodextrin) mixed biopolymers tested in tension. (b) Typical true stress/true strain curve obtained for the separated gelatin-rich matrix phase, originally from a gelatin continuous composition (12% (w/w) gelatin/12% (w/w) maltodextrin), demonstrating strain-hardening.

separated by 1.4 mm thick spacers, and cooled quickly to 5°C to prevent large scale phase separation. Samples were subsequently stored at this temperature for 24 h, prior to testing. All of the compositions examined in the current work lie within the immiscibility domain of the LH1e-SA2e-H_2O phase system [7], with the continuous and included phases each containing a small fraction of the other biopolymer [7]. For simplicity, each phase will in future be referred to by the major constituent biopolymer.

After storage, samples were cut from the gel sheets using a 'dog-bone' shaped cutters (60 mm gauge length and 6 mm width). Samples were then gripped using double-sided tape, stuck to cardboard tabs, in order to minimise handling damage. Tension tests were performed at a displacement rate of 50 mm min^{-1} (Instron 4502, High Wycombe, UK). True stress, σ_t, and true strain, ε_t, were calculated following;

$$\sigma_t = F(L_0 + \Delta L)/(A_0 L_0) \quad (1)$$

and

$$\varepsilon_t = \ln((L_0 + \Delta L)/L_0) \quad (2)$$

where F is the applied load, ΔL is the change in gauge length, and L_0 and A_0 are the initial gauge length and gauge section cross-sectional area, respectively. There was no evidence of localised necking during tensile testing of these materials.

Dynamic mechanical tests were also performed in situ on the CLSM, using a tension/compression stage (Minimat, Rheometric Scientific, Epsom, UK), using 'dog-bone' shaped samples (30 mm gauge length and 3 mm width due to stage size constraints). Due to stage vibration, real time dynamic video recording of the tests was not possible. Consequently, stepped tensile displacements were used (typically 2 mm at a rate of 10 mm min^{-1}), with an image acquired after each step. This procedure was repeated until the sample failed, after which further images were recorded of the relaxed microstructure.

A simple notched compact tension (CT) test was also developed to examine crack/microstructure interactions, adapted from tests developed for fracture energy determination [8]. Rectangular samples were used (30 mm long × 20 mm wide) with a side notch, perpendicular to the loading axis, of ~5 mm depth. Fracture energies were not determined using this configuration, in the current work. For the CT experiments, the notched samples were subjected to small stepped tensile displacements (typically 0.1 mm steps at 2 mm min^{-1}), while observing the notch tip on the CLSM. Eventually a crack propagates from the notch tip and grows in a stable manner. Further stepped displacements were then usually unnecessary. Crack advance was followed 'real time' on the CLSM, and recorded directly to video. Still images were subsequently captured from the video. For the micrographs presented in the present paper, the gelatin-rich phase appears light (due to the addition of the fluorescent stain), while the maltodextrin-rich phase appears dark.

3. Results and discussion

Typical true stress/true strain curves for gelatin/maltodextrin composites are shown in Fig. 1(a). Maltodextrin continuous samples (i.e. when gelatin is the included particle phase) show brittle behaviour, with an initially linear elastic response followed by catastrophic failure. Conversely, when the phase structure is inverted (i.e. gelatin continuous/maltodextrin included), the composite exhibits a novel 'pseudo-yielding' behaviour. This contrasts with *pure* gelatin gels of a similar concentration, which exhibit strain-hardening deformation in both compression and shear [9], as well as uniaxial tension [10]. The density difference between the two phases in the present gelatin/maltodextrin composite system allows the gelatin-rich phase to be separated from the mixed solution, prior to gelation (which was

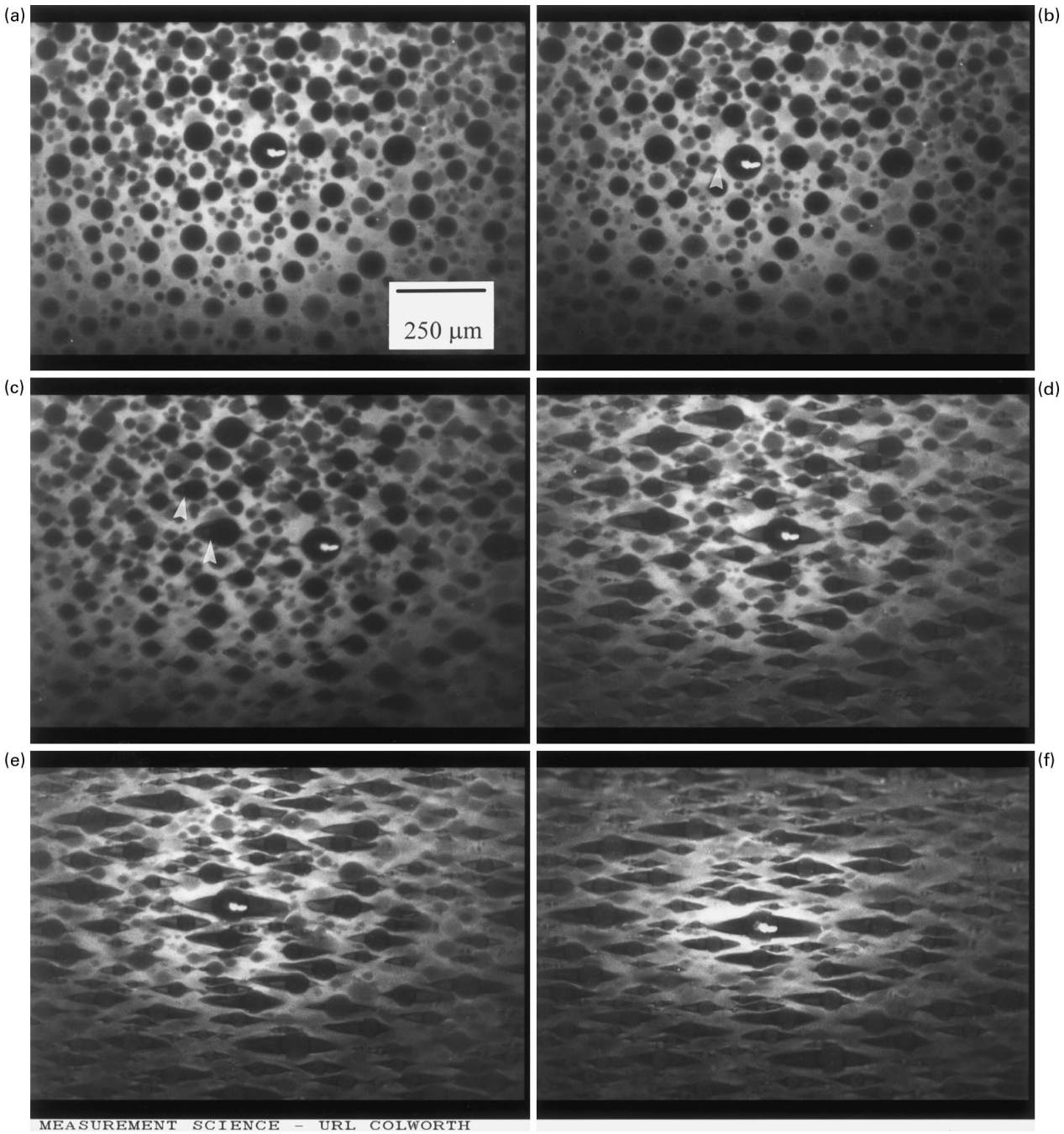

Fig. 2. Dynamic CLSM images of a tension test performed on a gelatin continuous sample (12% gelatin/12% maltodextrin), demonstrating the evolution of interfacial debonding (arrowed), and the subsequent formation of 'cusp' shaped voids, with increasing strain. Each image is taken from the same region of the sample and the deformation strains, calculated using Eq. (2), are: (a) 0.0 strain units; (b) 0.125; (c) 0.288; (d) 0.514; (e) 0.726; and (f) 0.818 (1.0 strain units is equivalent to 100% strain).

achieved by holding the sample at 60°C for 5 h). It is apparent that this phase alone also exhibits similar strain-hardening behaviour in tension (Fig. 1(b)) when the maltodextrin-rich included phase is removed. For deformation strains above that observed for *apparent* yielding, strain-hardening also occurs in the composite system (Fig. 1(a)), inferring that the continuous gelatin-rich phase dominates the mechanical response after debonding.

The 'pseudo-yielding' phenomenon of the gelatin continuous samples has been observed dynamically in tension, using the CLSM (Fig. 2). At strains above ~20%, debonding occurs at the interface between the maltodextrin particles and the continuous gelatin matrix (Fig. 2(c)), with subsequent void formation and growth. Debonding was occasionally observed at lower strains (~12.5%), between particles that are in close proximity, due to stress

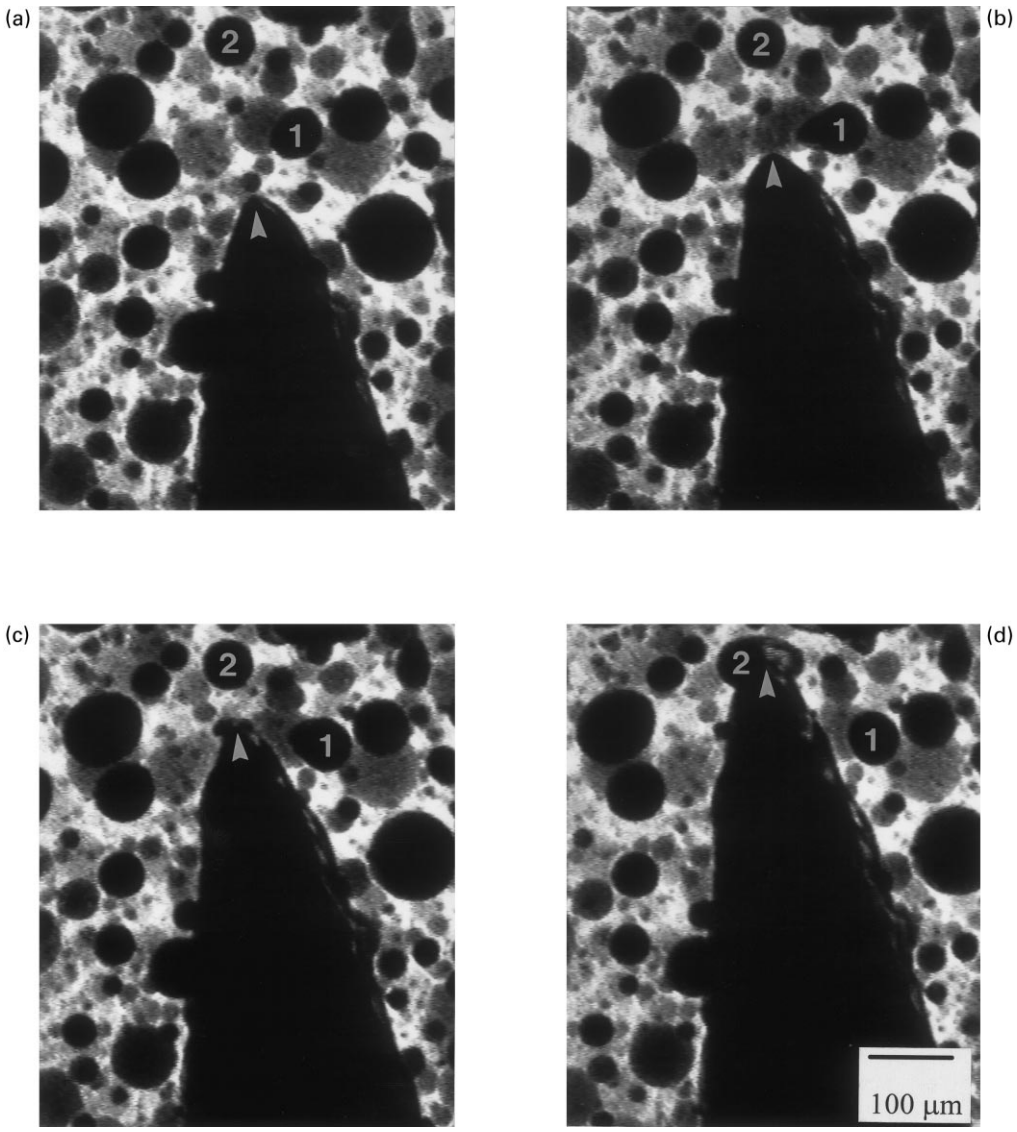

Fig. 3. Dynamic CLSM images of a notched tension test performed on a gelatin continuous composite sample (9.3% gelatin/8.0% maltodextrin): (a) Maltodextrin particle debonding is apparent ahead of the crack tip (i.e. particle 1); (b–d) with further crack advance maltodextrin particles are pulled out from the gelatin matrix (i.e. particle 2), while the strain around the debonded particle relaxes (particle 1).

concentration (Fig. 2(b)). Qualitatively, it can be seen that the larger included particles debond first. Such an observation is consistent with the debonding/void formation behaviour of elastomeric composites [11]. The interfacial fracture energy, G_c, can then be approximated, following;

$$\sigma_c^2 = 4\pi G_c E_m / 3r \quad (3)$$

if the debonding stress, σ_c, is known for a particle of radius, r, within a matrix of elastic modulus, E_m [11]. For the present example, debonding initially occurs at ~27 kPa for a particle diameter of ~100 μm and E_m ~75 kPa, corresponding to an interfacial fracture energy of ~0.25 J m^{-2}. This is an order of magnitude lower than typically observed for immiscible homopolymers (i.e. 1–5 J m^{-2}), without copolymer reinforcement [12,13], but similar to adhesion energies between glassy polymers (i.e. 0.05–0.5 J m^{-2}) [14,15]. It should be noted that all of these values are significantly less than the fracture energies for many pure polymers (i.e. 10^2–10^4 J m^{-2}) [8]. The approximate nature of the present analysis should be stressed, as the original model assumes non-interacting stress fields around each particle (i.e. a dilute system) [11].

Crack/microstructure interactions were assessed using the CT test geometry (Fig. 3). On a macroscopic level, the overall crack profile is relatively blunt, similar to that expected for conventional ductile materials [8]. Conversely, similar tests performed on maltodextrin continuous composites (i.e. gelatin included particles), showed a sharp crack profile [16], which is typical of brittle materials [8]. Fig. 3(a) demonstrates that debonding of the particle/matrix interface can occur ahead of the crack tip, due to stress concentration

in this region. As the crack advances, complete particles are 'pulled out' of the matrix on one side of the crack or the other. Post test examination of the failure surfaces revealed that the particles did not fracture, but remained intact, confirming the low interfacial fracture energy noted earlier.

In the present work, novel mixed biopolymer composites have been developed which exhibit a 'pseudo-yielding' stress/strain response. One of the unique aspects of this work is the utilisation of dynamic tension and notched tension tests, performed on a CLSM, to elucidate mixed biopolymer failure mechanisms. Using this approach it was shown that the yielding phenomenon could be attributed to particle/matrix interfacial debonding and the subsequent growth of 'cusp' shaped voids. Using a simple elastomer composite debonding model [11], an approximate interfacial fracture energy of $\sim 0.25\ J\ m^{-2}$ is calculated, comparable to weak glassy polymer interfaces. Future work will aim to confirm these measurements using the appropriate interfacial mechanical tests used for weak polymer interfaces [14,15], and also to determine the fracture energy of the bulk samples directly using a thin film plane stress work of fracture test [17].

Acknowledgements

The authors would like to thank Drs I.T. Norton, W.J. Frith, A.H. Clark and B. Wolf for valuable discussions and comments on biopolymer gels.

References

[1] Clark AH, Ross-Murphy S. Adv Polym Sci 1987;83:57.
[2] van Vliet T, Walstra P. Faraday Discussions 1995;101:359.
[3] Morris VJ. Chem Ind 1985;5:159.
[4] Brownsey GJ, Ellis HS, Ridout MJ, Ring SG. J Rheol 1987;31:635.
[5] Gao YC, Lelievre J. Polym Engng Sci 1994;34:1369.
[6] Normand V, Plucknett KP, Frith WJ, Pomfret SJ. Unpublished research.
[7] Normand V, Pudney PDA, Aymard P, Norton IT. Submitted for publication.
[8] Atkins AG, Mai Y-W. Elastic and plastic fracture: metals, polymers, ceramics, composites, biological materials, Chichester: Ellis Horwood, 1985.
[9] Groot RD, Bot A, Agterof WGM. J Chem Phys 1996;104:9202.
[10] Plucknett KP. Unpublished research.
[11] Gent AN. J Mater Sci 1980;15:2884.
[12] Creton C, Kramer EJ, Hui CY, Brown HR. Macromolecules 1992;25:3075.
[13] Kulasekere R, Kaiser H, Ankner JF, Russell TP, Brown HR, Hawker CJ, Mayes AM. Macromolecules 1996;29:5493.
[14] Gent AN, Shimizu N. J Appl Polym Sci 1986;32:5385.
[15] Mangipudi VS, Huang E, Tirrell M, Pocius AV. Macromol Symp 1996;102:131.
[16] Plucknett KP, Normand V, Ferdinando D. Unpublished research.
[17] Plucknett KP, Normand V. In preparation.